# Histomorphological Study of the Meibomian Glands in New Zealand White Rabbits (*Oryctolagus cuniculus*): A Light Microscopic Investigation

**Tareq Ziad Khalaf [1], Farqad R. Faihan[2]**

[1,2] Department of Medical Laboratory Techniques, College of Health and Medical Techniques,University of Al-Maarif, Ramadi, Iraq.
Email: tareq.ziad@uoa.edu.iq[1], farqad.Riyadh@uoa.edu.iq[2]

**ABSTRACT**

**Background and Objective**: The meibomian glands are specialised holocrine sebaceous glands that are encapsulated within the tarsus of the eyelids in domestic animals. The secretion of these glands, called meibum, is important for the stability of the precorneal tear film and for the health of the ocular surface. While the clinical and veterinary significance of these glands has been established, there are no detailed histological or morphometric studies available for New Zealand White rabbits (Oryctolagus cuniculus). The objective of this study was to identify the histomorphological features of meibomian glands in this breed and to provide quantitative morphometric data related to the number of meibomian glands between eyelid positions (i.e. upper and lower) and between male and female rabbits.

**Materials and Methods**: Eyelid specimens were collected from ten clinically normal New Zealand White rabbits (5 males, 5 females; 10-14 months old; 3-5 kg) immediately after slaughter. The specimens were fixed in 10% buffered formalin for 72 hours and processed using standard histological techniques. Tissue sections (5µm) were stained using the Hematoxylin and Eosin (H&E), Periodic Acid- Schiff (PAS), and Masson's Trichrome staining protocols and examined with a light microscope.

**Results**: The mean number of meibomian glands from both the left and right upper eyelids (27.4±0.3 and 26.8±0.4) was significantly greater ($P<0.001$) than the mean number of meibomian glands from both the left and right lower eyelids (21.3±0.2 and 20.6±0.2). No significant differences in laterality or sex were observed. Histologically, the meibomian glands contained multiple branched acini leading into short ductules that connected to one central excretory duct. Lipocytes in the meibomian glands contained numerous cytoplasmic vacuoles, consistent with holocrine secretion. PAS staining revealed a continuous basement membrane around the meibomian glands, and Masson's Trichrome staining demonstrated collagen surrounding the ducts.

**Conclusions**: The histomorphological features of meibomian glands in New Zealand White rabbits are similar to those reported in other domestic species and differ from those reported for other domestic species. These findings provide baseline reference data for veterinary ophthalmology researchers and for clinicians who provide services to laboratory animal species.

**Keywords:** meibomian gland; *Oryctolagus cuniculus*; histomorphology; New Zealand White rabbit; holocrine secretion; tear film; tarsal gland; eyelid

## Introduction

The eyelid is an important and complex structure that supports many of the functions vital to the overall health of the eyes and the ocular adnexa. An eyelid consists of four distinct tissue layers: the superficial skin layer containing fine hairs and sebaceous glands; the striated muscle layer responsible for closing the eyelid; the fibrous tarsal plate that provides rigidity and support to the eyelid; and the palpebral conjunctiva, which is continuous with the bulbar conjunctiva and attaches to the globe of the eye. [1,2] Embedded within the tarsal plate are the meibomian glands (also called tarsal glands), which are the largest glands within the eyelid and are also the most visible. Meibomian glands were first observed by Heinrich Meibom in 1666, and the fascinating study of these glands has generated great interest in veterinary and human medicine alike. [3,4]

The meibomian glands are morphologically classified as modified or enlarged sebaceous glands and are different from typical sebaceous glands in that they do not have associated hair follicles. [5,6] Each meibomian gland contains several branching acini, which are arranged radially around a single central excretory duct that runs the entire length of the tarsal plate. The acini communicate with the excretory duct through short, narrow ductules, and the central duct opens ontoQ the eyelid margin through an orifice that lies along the mucocutaneous junction and behind the row of cilia on the upper eyelid. Human beings are endowed with a varying range of meibomian glands that are determined by both the size of the palpebral aperture as well as the width of the tarsal plate [7,8].

On average, there are between 25 and 40 meibomian glands in the upper eyelids and 20 and 30 meibomian glands in the lower eyelids. In terms of cellular arrangement, the meibomian glands comprise two main cell populations: a peripheral basal layer and a central ductal layer [9]. The peripheral basal layer comprises undifferentiated, mitotic

progenitors (mitotic cells have darkly stained nuclei and little cytoplasm) that lie atop a continuous basement membrane [10]. The cells in the middle (central ductal layer) progress through multiple (successive) generations of differentiation until they reach full maturity and accumulate intracellular lipid droplets in their cytoplasmic space [11,12]. Once these cells reach full maturity, their cytoplasm is replaced by lipid droplets, and they subsequently undergo programmed cell death [13]. The cytoplasmic lipid droplets are then released into the ductal lumen by holocrine secretion. The rate of meibum secretion, a complex oily substance with viscous properties, depends on many factors, including hormonal regulation, neural control, and environmental conditions [14,15]. The secretory product of the meibomian glands is known as meibum, which forms the outer lipid layer of the three-layered precorneal tear film. Chemically, meibum is composed of many different types of lipids, including wax monoesters, sterol esters, and (O-acyl)-omega-hydroxy fatty acids, all of which provide different physical properties for the lipid film [16]. The meibomian gland's lipid layer is mainly responsible for keeping tears from evaporating, reducing tension on the tear film, and preventing tears from running off the eyes onto the skin. [9,17] In general, the stratum granulose and stratum corneum are not well-developed along the length of a meibomian gland's duct. The distal part of the duct, close to the eyelid opening, may develop both strata, setting it apart from the eyelid's more keratinised epidermis. [10,18]

Dry eye disease from evaporation is a major cause of dry eyes globally; drying out the eye so the meibomian gland does not produce enough tears leads to MGD [19], which causes the glands to stop producing oil and causes keratinisation of the ducts; these changes cause instability in the lipid layer of the tear film, where excess water evaporates from the tear film. This leads to higher salt concentrations in tears, damage to epithelial cell membranes, and chronic inflammation of the ocular surface. These changes have major effects on both animal welfare and productivity in livestock. [1,3]

Morphological studies of meibomian glands from different mammals have greatly aided the understanding of the structure-function relationships in this tissue. Jester et al. investigated the histology and ultrastructure of rabbit meibomian glands and presented an experimental model of MGD, which has contributed to further research on MGD treatment. [5,20] Investigations of meibomian lipid composition in bovine species (Steers) were completed, and the lipid content of bovine meibomian secretion was compared to the lipid content of human meibomian secretion. It was determined that non-polar lipid classes differ significantly between species. [15] Horse, dog, and cat meibomian glands have been reviewed in a veterinary context, with these species showing meibomian gland architecture similar to that of all mammals. [21,22] For laboratory mammals, there are few available histomorphologic studies examining the structure of meibomian glands in rabbits. Jesters et al. cited the need for histomorphological investigation of meibomian glands. The only example of a genus in laboratory mammals in which histomorphology of meibomian glands has been documented is Shrew (Suncus murinus viridescens), where meibomian glands were present at the eyelid margins of both the upper and lower eyelids of male and female animals, demonstrating significant conservation of meibomian glands across most genera of mammals. [23] In veterinary and laboratory animal practice, conditions affecting meibomian glands in rabbits have been reported; however, given that normative histomorphological data for the New Zealand White rabbit (Oryctolagus cuniculus) are absent, the evaluation of any pathologic change of a rabbit's meibomian glands will be dependent on reliable equipment that provides adequate accuracy and reliability. [21,22]

The New Zealand White rabbit is a widely used model in biomedical and ophthalmic research, and through ocular health, rabbit welfare and utility as a research subject are of considerable importance. Yet, despite the importance of this rabbit breed, there has yet to be a dedicated histomorphological evaluation of meibomian glands in the New Zealand White rabbit. The absence of such research represents a considerable deficiency in our current foundational understanding of the morphological characteristics of this breed and in advances in comparative ophthalmic research and veterinary diagnostics. [24,25] Therefore, this study is designed to provide a comprehensive histomorphological characterisation of the meibomian glands in the New Zealand White rabbit using light microscopy with H&E (Hematoxylin and Eosin), PAS (Periodic Acid Schiff) and Masson Trichrome staining, in combination with an assessment of the number of meibomian glands located at each eyelid position, and those located on each sex of rabbit.

## Materials And Methods

### Animals and Tissue Collection

Ten clinically normal New Zealand White rabbits were included: half male and half female, aged between 10 and 14 months, with weights ranging from 3 kg to 5 kg. All rabbits were raised under standard laboratory conditions until euthanasia. At the time of euthanasia, there was no evidence of any disease (ocular/systemic) based on a veterinary clinical examination before death. The eyelid specimens were collected immediately following euthanasia (15–20 minutes post-mortem) to minimise postmortem autolysis. For the collection of whole eyelids, both upper and lower eyelids from each left and right eye were dissected, preserving the integrity of the tarsal plate and associated glands using precise dissection techniques. A total of four eyelid specimens were taken from each rabbit, resulting in 40 eyelid specimens collected for analysis within this study. All specimens were labelled individually and sent to a histology laboratory for storage at low temperatures.

### Tissue Fixation and Histological Processing

After being collected, dissected specimens were fixed in neutral-buffered formalin (pH 7.2-7.4) at 20°C for 72 hours. After the fixation was finished, each dissected specimen was cut to include the entire thickness (from the outer skin

layer to the inner layer of the eyelid) and to preserve the tarsal plate. The tissue from the dissected specimens was processed using an established histology routine. The processing included sequentially immersing the tissue in graded alcohols for the initial drying (i.e., 70% ethanol, 80% ethanol, 95% ethanol, and two changes in absolute ethanol). The second step in the processing was the use of xylene (two changes) to clear the dried tissues; paraffin was the last step in the histological processing, which involved embedding the cleared dried tissue blocks in hot paraffin wax (60 degrees Celsius for two changes). The tissue sections are oriented to a specific tissue sectioning plane; hence, cross-sectional cuts were made along the long axis of the acinus and central duct.

**Sectioning**

Using a calibrated rotary microtome (Leica RM2125, Leica Biosystems), serial sections approximately 5 µm thick were prepared and floated onto albumin-coated microscope slides. The slides were subsequently placed on a 37°C warming plate overnight to ensure adequate section attachment for staining. Each specimen had five representative sections assigned to each staining protocol, allowing independent assessments of general structures, mucopolysaccharide distribution, and types of connective tissue components.

**Histochemical Staining**

Three established histochemical staining methods were employed: Haematoxylin and Eosin (H&E), Periodic Acid-Schiff (PAS), and Masson's Trichrome.

Haematoxylin and Eosin staining was performed using Harris haematoxylin, with differentiation in 1% acid alcohol and bluing in Scott's tap water substitute, followed by counterstaining with eosin-phloxine solution. This protocol provided an optimal demonstration of the general histological architecture, including nuclear morphology, cytoplasmic characteristics, and cellular organisation within the acini and excretory ducts. [26,27]

Periodic Acid-Schiff staining was used to demonstrate the basement membrane surrounding the acini as well as any mucopolysaccharide-rich components within the glandular epithelium and stroma. Sections were oxidised with 1% periodic acid for 10 minutes, rinsed, exposed to Schiff's reagent for 15 minutes, and then counterstained with haematoxylin. PAS-positive material was identified by the characteristic magenta colouration produced upon oxidation of vicinal diol groups in polysaccharide chains. [26,27]

Masson's Trichrome staining was applied for the specific demonstration of collagen fibres within the interacinar and periductal stroma. The protocol involved sequential treatment with Weigert's iron haematoxylin, Biebrich scarlet-acid fuchsin solution, phosphomolybdic–phosphotungstic acid, and aniline blue, resulting in the staining of collagen fibres in blue, muscle fibres and cytoplasm in red, and nuclei in dark brown. [26,27]

**Microscopic Examination and Morphometrics**

Using an Olympus BX41 binocular light microscope (Japan), we analysed all sections stained at magnifications of ×40, ×100, and ×400. The average count of meibomian glands in the eyelid was determined by systematically counting their locations on at least three randomly selected representative sections per specimen at a lower magnification; this information was reported as the mean and standard error of the mean (±SEM). To compare data on meibomian gland counts among the upper and lower lids, between left and right eyes, and among males and females, we used independent-samples t-tests for nondependent variables and paired-samples t-tests for dependent variables in IBM SPSS Statistics, version 26. A p-value of less than 0.05 was determined to indicate statistical significance.

## Results

**Gross Anatomical Observations**

Upon visual inspection, Meibomian glands in New Zealand White rabbits were identified as distinct pale yellowish-white bands, arranged parallel to one another and oriented at right angles to the free border of the eyelids, on the inner (conjunctival) surface of both the upper and lower eyelids. Adult rabbits exhibited white/cream coloured Meibomian glands located just beneath the palpebral conjunctiva of the eyelids within the tarsal plates. The openings of the central excretory ducts all followed a straight line along the edge of the eyelid. No gross morphological differences existed between the male and female, or the left and right eyelids.

**Morphometric Findings: Meibomian Gland Number**

Using morphometric analysis, it was shown that there were more meibomian glands in the upper eyelid than in the lower eyelid in every animal examined ($p < 0.001$). The average number of glands per animal is provided in Table 1. No statistically significant differences were observed between the left and right sides for any location ($p > 0.05$) or between the males and females for any location ($p > 0.05$), as indicated in Table 3.

**Table 1. Mean number of meibomian glands (Mean ± SEM) by eyelid position in New Zealand White rabbits (n=10)**

| Eyelid Position | Mean ± SEM | Range | p-value vs Lower eyelid |
|---|---|---|---|

| | | | |
|---|---|---|---|
| Upper Left | 27.4 ± 0.3 | 26 – 29 | < 0.001 |
| Upper Right | 26.8 ± 0.4 | 25 – 28 | < 0.001 |
| Lower Left | 21.3 ± 0.2 | 20 – 22 | — |
| Lower Right | 20.6 ± 0.2 | 19 – 21 | — |

*SEM: standard error of the mean. p-values represent the comparison of the upper vs the lower eyelid by an independent samples t-test.*

**Histological Findings by H&E Staining**

H&E staining of the sections revealed that the meibomian glands of New Zealand White rabbits possess many branched acini with a single, noticeable central duct via short ductules located among a dense connective tissue structure (tarsal plate) (see Figures 1 and 2). The outer layer of each acinus contained flat, roundish basal cells with little indication of "differentiation", large oval, basophilic nuclei, and a little eosinophilic cytoplasm. In contrast, the inner layer of lipocyte-type cells contained larger intracellular lipid vacuoles closer to the duct. These large, fat-filled vacuoles increase in size as lipocytes "mature" and approach the ductal lumen. In mature cells, the cytoplasm consists almost entirely of vacuoles filled with lipids. The central excretory duct is covered with a multilayered squamous type of epithelium, and as the epithelium nears the opening at the end, there is an increase in keratinisation. The palpebral conjunctiva can easily be seen as a thin layer of multilayered epithelium on the eyelid's inner surface. Bundles of orbicularis oculi muscle tissue can be found in the deep tissue of the eyelid.

*Figure 1. Photomicrograph of meibomian gland acini in New Zealand White rabbit eyelid (Masson's Trichrome, ×100). Multiple branched acini are seen opening toward the central excretory duct (top). Peripheral basal cells with darkly stained nuclei line each acinus, and vacuolated lipocytes are visible centrally. Collagen fibres appear in the interacinar stroma.*

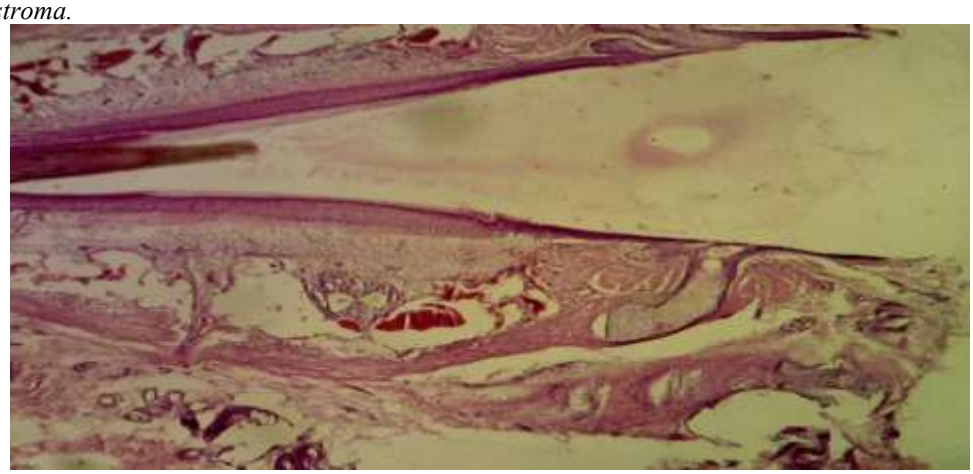

*Figure 2. Low-power photomicrograph of the eyelid showing the overall organisation of meibomian gland units within the tarsal plate (H&E, ×40). The palpebral conjunctiva is visible as the thin epithelial lining at the upper aspect. Glandular ductal structures (pale spaces) and associated acinar clusters are clearly delineated within the connective tissue stroma. Blood vessels are present in the sub-glandular tissue.*

**Histological Findings by Masson's Trichrome Staining**

Collagen fibres stained blue were also identified throughout the acinar interstitial spaces connecting adjacent acini, forming denser concentric rings surrounding the central excretory duct. In addition to collagen fibres, the orbicularis oculi muscle fibres stained red, providing a visual distinction between the muscles and glands of the tarsal plate and thereby validating the anatomical orientation of the histological sections. Acinar epithelial cells were identified by their red-stained cytoplasm, while the nuclei of basal cells were stained dark brown by Weigert's iron haematoxylin. **Table 2** summarises histomorphological observations obtained with all three staining methods.

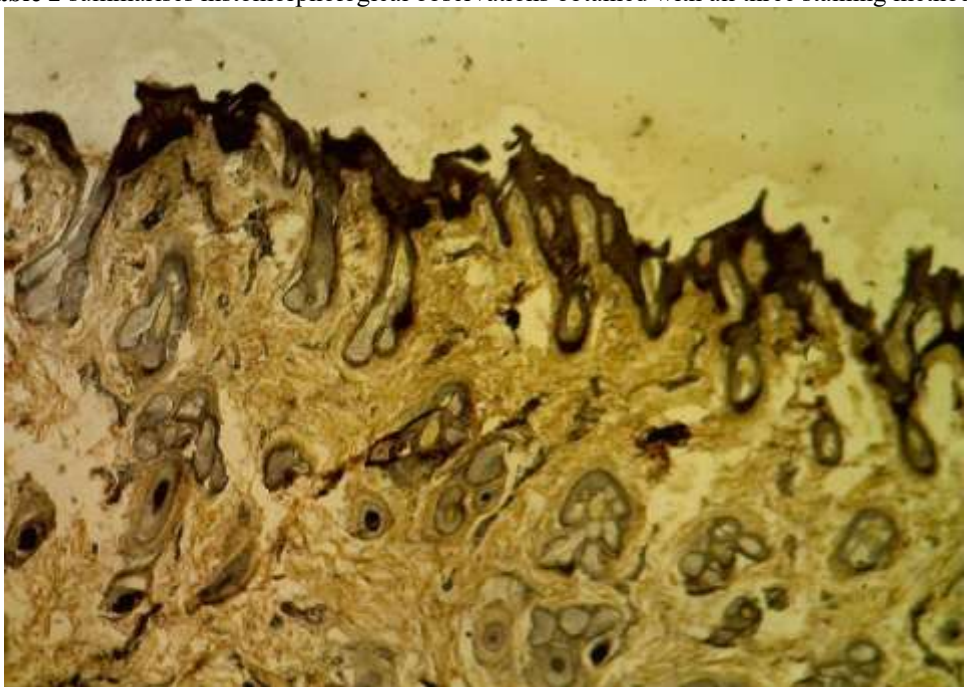

*Figure 3. Photomicrograph of meibomian gland acini in New Zealand White rabbit eyelid at medium magnification (Masson's Trichrome, ×100). Numerous cross-sections of branched acini are visible, each surrounded by blue-staining collagen fibres. The palpebral conjunctival surface is seen at the upper margin. The acinar units display a clear distinction between the peripheral basal cells and the centrally vacuolated mature lipocytes.*

**Table 2. Summary of histomorphological features observed in meibomian glands of New Zealand White rabbits across three staining methods**

| Staining Method | Principal Structures Demonstrated | Key Findings |
|---|---|---|
| H&E | General morphology; nuclear and cytoplasmic detail | Branched acini; peripheral basal cells with oval haematoxyphilic nuclei; central lipocytes with large vacuolated cytoplasm; stratified squamous ductal epithelium becoming keratinised at the lid margin |
| PAS | Basement membrane; mucopolysaccharides | Strongly PAS-positive continuous basement membrane surrounding each acinus; weak PAS reactivity in superficial ductal epithelium; lipocyte cytoplasm PAS-negative |
| Masson's Trichrome | Collagen fibres; muscle fibres; connective tissue organisation | Dense blue-stained collagen in periductal stroma; moderate collagen in interacinar septa; muscle fibres of orbicularis oculi stained red; acinar cytoplasm red |

*H&E: Haematoxylin and Eosin; PAS: Periodic Acid-Schiff.*

**Histological Findings by H&E Staining — Longitudinal Architecture**

Figure 4 shows the meibomian gland unit in the lower eyelid of a New Zealand White rabbit; each section from this photograph was taken using low magnification. This image illustrates how the central duct connects with the acinar clusters surrounding it and has a defined border with the fibrous tarsal plate, which forms the boundary between the inner surface of the upper eyelid (palpebral) conjunctiva and the outer surface of the fibrous tarsal plate, and is

conspicuously outlined. The acinar clusters are arranged in a lobular pattern, with each being located on opposite sides of the duct. The presence of moderate amounts of loose connective tissue between the adjacent lobular structures of the glands provides some stability to the architecture of the tarsal plate.

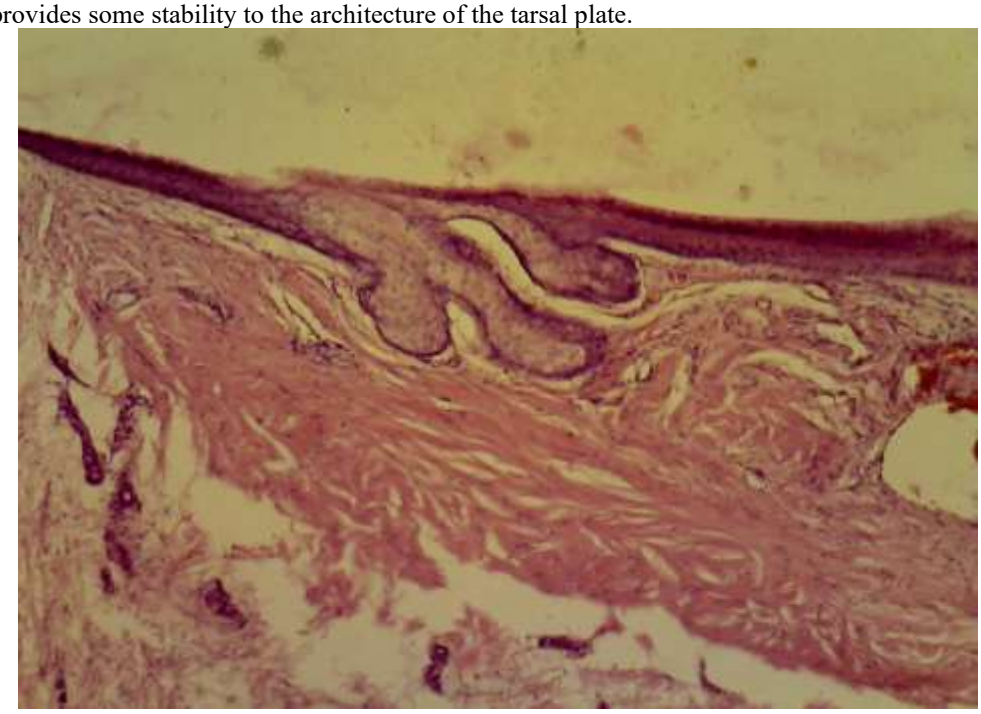

*Figure 4. Low-power photomicrograph of a longitudinal section through the lower eyelid of a New Zealand White rabbit (H&E, ×40). The palpebral conjunctiva (top, dark band) overlies the dense fibrous tarsal plate. Meibomian gland acini and the central excretory duct are visible as structured pale lobules within the fibrous tissue. Bundles of fibrous connective tissue and blood vessels occupy the sub-glandular space.*

**Table 3. Mean number of meibomian glands (Mean ± SEM) by sex and eyelid position in New Zealand White rabbits**

| Eyelid Position | Males (n=5) Mean ± SEM | Females (n=5) Mean ± SEM | p-value | Combined Mean ± SEM |
|---|---|---|---|---|
| Upper Left | 27.6 ± 0.4 | 27.2 ± 0.4 | 0.472 | 27.4 ± 0.3 |
| Upper Right | 27.0 ± 0.5 | 26.6 ± 0.6 | 0.617 | 26.8 ± 0.4 |
| Lower Left | 21.4 ± 0.3 | 21.2 ± 0.3 | 0.688 | 21.3 ± 0.2 |
| Lower Right | 20.7 ± 0.2 | 20.5 ± 0.2 | 0.476 | 20.6 ± 0.2 |

*No statistically significant sex differences were detected at any eyelid position (all $p > 0.05$ by independent samples t-test).*

## Discussion

This article provides the first systematic histomorphological report on the Meibomian glands in New Zealand White rabbits (Oryctolagus cuniculus). It employs three distinct histochemical staining methods, along with a quantified morphometric assessment of Meibomian gland number. The results show that, despite the morphological similarity of the Meibomian glands of this breed to the general mammalian pattern observed in other domestic animals, the quantitative data on the number of Meibomian glands per eyelid position provide new species-specific reference values with practical implications for veterinary ophthalmology and comparative biology. [1,4]

The values for the mean number of Meibomian glands for this study are 27.4 ± 0.3 for the upper eyelids and 26.8 ± 0.4 for the upper eyelids, and 21.3 ± 0.2 for the lower eyelids and 20.6 ± 0.2 for the lower eyelids, showing a consistent, significant asymmetry of the means for the upper and lower eyelids, with the upper eyelid having a much greater number of Meibomian glands than the lower eyelid. This asymmetry is biologically reasonable in terms of the larger upper tarsal plate sizes when compared to the smaller lower tarsal plates in the majority of domestic mammals, because the longer vertical distance of the upper eyelid permits the upper eyelid to have a larger quantity of Meibomian gland units. [4,11] The same upper to lower asymmetry has frequently been documented in human beings, where the upper eyelid has 25-40 Meibomian glands, while the lower eyelid has 20-30 Meibomian glands, with the ratio of upper to lower glands in humans being similar to that of rabbits in this study. [4,8]

The absolute Meibomian gland numbers observed in rabbits compared to humans may reflect the differences in palpebral aperture dimensions and tarsal plate size in rabbits, which require a commensurate number of Meibomian glands to maintain a proper lipid film across the exposed ocular surface.

The absence of statistically significant differences in gland number between the left and right eyelids is consistent with the bilateral symmetry expected of an evenly developed anatomical structure and corroborates findings in other species studied. [4,20] Similarly, the lack of significant sex-related differences in meibomian gland number between male and female rabbits suggests that gland number in this species is primarily determined by the dimensions of the tarsal plate rather than by hormonal influences. This contrasts with findings from some human studies suggesting that androgens influence meibomian gland secretory activity; however, such effects are generally more pronounced in adults with marked sexual dimorphism than in juvenile rabbits in the age range studied here. [13,24]

The meibomian glands show the usual histological structure found in H&E-stained tissue sections (Figures 1 and 2). These glands are composed of numerous branched acini that converge via short ductules on a common long central excretory duct. There is a close resemblance in the structure of meibomian glands described for rabbits by Jester et al. [5,14]. These glands contain acinar lobules with undifferentiated basal cells at their periphery and lipid-laden sebocytes centrally located within the lobule, which undergo progressive differentiation and eventual disintegration via holo-crine secretion. [7,8]. In H&E-stained sections of rabbit meibomian glands, the large lipid vacuoles in mature lipocytes represent holocrine secretory cells and form as a result of the dissolution of neutral lipid droplets during processing; these vacuoles are termed ghost cells or vacuolated lipocytes in the histological literature. [8,14]. Ductal epithelium of the meibomian glands shows a transition of the non-keratinised stratified squamous epithelium, which is present proximally, to a keratinised type of epithelium near the lid margin orifice. This is a characteristic feature of all mammals, as a mechanical barrier at the terminal duct contacts the physical environment at the lid margin. [10,18]

The Masson's Trichrome results shown in Figure 3 illustrate the connective tissue structure of the rabbit meibomian gland region. The abundance of collagen fibres surrounding and between the acini of the rabbit meibomian glands is consistent with that of the tarsal plate in domestic mammals, where the dense, regular connective tissue provides mechanical support and a framework in which to embed the glandular units. Studies have proposed that the collagen fibre network of the meibomian glands provides the compressive force needed to propel meibomian secretions along the ductal system during representative physiological actions, such as blinking. [3,17] To assist in evaluating the morphological characteristics of the Tarsal Plate, clear evidence of muscle fibre delineation through red staining enabled the researchers to validate that their Tarsal Plate specimens were appropriately oriented anatomically. [3,17] The data obtained from this study support similar findings for bovine and equine specimens captured within the veterinary literature. [15,21]

Based upon the PAS results, it was determined that there was a strong positive (PAS+) and well-defined basal lamina on each acinus; this structure, containing an abundance of glycoproteins, is found in all glandular epithelium, separates the connective tissue from the secretory epithelium and is necessary for structural integrity and regenerative capability of the acini. [9,26] In contrast to the above findings, it is expected that the cytoplasm of mature lipocytes will be largely PAS- due to the absence of diol groups required for reactivity with PAS, explaining the differences observed between PAS staining of the meibomian lipocytes versus conjunctival goblet cells (strong PAS staining). [14,27] Moderately weak to the PAS reaction observed in the superficial ductal epithelial layers may represent either the presence of glycoprotein material in the epithelial cell membranes or glycoprotein components of the superficial ductal epithelial layer (e.g., glycoproteins providing lubricating properties to the ducta1 cavity). Figure 4 is a longitudinal view of a rabbit's lower eyelid in low power and illustrates the positional relationship of the conjunctiva, tarsal plate, and meibomian gland units. The arrangement of the acinar clusters into lobules, with respect to the central duct, coincides with the excretory duct extending the entire length of the tarsal plate and is consistent with classical anatomy descriptions of meibomian glands from domestic animal species. [4,11] The fibrous nature of the tarsal plate in rabbits is comparable to the structural organisation of the tarsal plates of other mammalian species. It indicates the need for the tarsal plate to support the eyelid's mass and length. [21,22]

The meibomian gland secretory process is clearly identified as holocrine. Therefore, the development of cytoplasmic lipid vacuoles from peripheral basal cells toward central, closely packed, mature sebocytes, and their ultimate degeneration and release of lipids into the duct lumen, correspond exactly to the definition of holocrine secretion in histological nomenclature. [7,11,12] The importance of defining the meibomian glands as holocrine applies to understanding the pathology of meibomian gland function. For example, because the basal layer of peripheral cells continues to regenerate, the absence of basal cell proliferation in pathological conditions such as inflammation, age-related acinar degeneration, and toxin exposure may cause permanent loss of meibomian gland function and partial inability to secrete lipids. [24,28]

The results of this study are relevant to veterinary clinical practice and can assist veterinary and research diagnostic practitioners in interpreting eyelid biopsy results in rabbits. The counts of glands found on biopsy are particularly helpful for evaluating atrophy or hyperplasia of the meibomian glands in rabbits, as they must be compared with healthy controls matched for age and sex to make an accurate diagnosis. [16,17] Future studies utilising in vivo infrared meibography similar to that reported for humans and dogs could be conducted to investigate meibomian gland function in live animals while also generating longitudinal data to support the ex vivo histomorphological findings from this study. Additionally, ultrastructural studies using transmission electron microscopy could be performed to

clarify further the fine cellular structure of the basal cell layer and the mechanisms of lipid secretion from that layer in this species. [30]

## Conclusion

This study is the first to examine the Meibomian glands (MG) of New Zealand White rabbits (Oryctolagus cuniculus) using light microscopy with H&E, PAS, and Masson's Trichrome stains. The MGs are modified holocrine sebaceous glands that lack follicles and occupy the tarsal plate; they are composed of many branched acini that open into a single long excretory duct. The photomicrographs provide, for the first time, histological evidence of the MG architecture, vacuolated lipocyte morphology, collagen arrangement surrounding the duct(s), and the lobular configuration of acini within the tarsal plates of this breed. The number of MG is significantly higher in the upper eyelids (mean 27.4 left, 26.8 right) than in the lower eyelids (mean 21.3 left, 20.6 right), with no significant differences by sex or laterality. This data serves as a foundation for veterinarians and researchers studying meibomian gland disease and function in this rabbit breed and establishes a normative reference for veterinary ophthalmologists and other research professionals conducting clinical or comparative studies of the MG in laboratory rabbits.

**Conflict of Interest:** The authors declare no conflicts of interest.

**Funding:** This research received no external funding.

## References

1. Driver PJ, Lerap MA. Meibomian gland dysfunction. Surv Ophthalmol. 1996;40(5):343-67.
2. Knop E, Knop N, Millar T, Obata H, Sullivan DA. The international workshop on meibomian gland dysfunction: report of the subcommittee on anatomy, physiology, and pathophysiology of the meibomian gland. Invest Ophthalmol Vis Sci. 2011;52(4):1938-78.
3. Bron AJ, Tiffany JM. The contribution of meibomian disease to dry eye. Ocul Surf. 2004;2(2):149-65.
4. Knop N, Knop E. Meibomian glands: part I: anatomy, embryology and histology of the meibomian glands. Ophthalmologe. 2009;106(10):872-83.
5. Jester JV, Rife L, Nii D, Luttrull JK, Wilson L, Smith RE. In vivo biomicroscopy and photography of meibomian glands in a rabbit model of meibomian gland dysfunction. Invest Ophthalmol Vis Sci. 1982;22(5):660-7.
6. Fuchs E. Skin stem cells: rising to the surface. J Cell Biol. 2008;180(2):273-84.
7. Junqueira LC, Carneiro J. Basic Histology: Text and Atlas. 10th ed. New York: McGraw-Hill; 2003.
8. Thody AJ, Shuster S. Control and function of sebaceous glands. Physiol Rev. 1989;69(2):383-416.
9. Ehlers N. The precorneal film: biomicroscopical, histological, and clinical investigations. Acta Ophthalmol Suppl. 1965;81:1-134.
10. Elias PM, Goerke J, Friend DS. Mammalian epidermal barrier layer lipids: composition and influence on structure. J Invest Dermatol. 1977;69(6):535-46.
11. Wolff E, Warwick R. Anatomy of the Eye and Orbit. 7th ed. Philadelphia: WB Saunders; 1976. p. 194-6.
12. Mathers WD, Shields WJ, Sachdev MS, Petroll WM, Jester JV. Meibomian gland morphology and tear osmolarity: changes with Accutane therapy. Cornea. 1991;10(4):286-90.
13. Sullivan DA, Dartt DA, Meneray MA, editors. Lacrimal Gland, Tear Film, and Dry Eye Syndromes 2: Basic Science and Clinical Relevance. New York: Plenum Press; 1998.
14. Jester JV, Nicolaides N, Smith RE. Meibomian gland studies: histologic and ultrastructural investigations. Invest Ophthalmol Vis Sci. 1981;20(4):537-47.
15. Nicolaides N, Kaitaranta JK, Rawdah TN, Macy JI, Boswell FM, Smith RE. Meibomian gland studies: comparison of steer and human lipids. Invest Ophthalmol Vis Sci. 1981;20(4):522-36.
16. Bron AJ, Benjamin L, Snibson GR. Meibomian gland disease: classification and grading of lid changes. Eye. 1991;5(Pt 4):395-411.
17. Gutgesell VJ, Stern GA, Hood CI. Histopathology of meibomian gland dysfunction. Am J Ophthalmol. 1982;94(3):383-7.
18. Tiffany JM. Individual variations in human meibomian lipid composition. Exp Eye Res. 1978;27(3):289-300.
19. Norn MS. Meibomian orifices and Marx's line: studied by triple vital staining. Acta Ophthalmol. 1985;63(6):698-700.
20. Samuelson DA. Ophthalmic anatomy. In: Gelatt KN, editor. Veterinary Ophthalmology. 3rd ed. Baltimore: Lippincott Williams & Wilkins; 1999. p. 31-150.
21. Gelatt KN, editor. Veterinary Ophthalmology. 4th ed. Ames: Blackwell Publishing; 2007.
22. Gelatt KN, Ben-Shlomo G, Gilger BC, Hendrix DV, Kern TJ, Plummer CE. Veterinary Ophthalmology. 5th ed. Ames: Wiley-Blackwell; 2013.
23. Quay WB. Integument and the environment: gland and hair in adaptation and defense. Am Zool. 1977;17(1):119-33.
24. Blackie CA, Korb DR, Knop E, Bedi R, Knop N, Holland EJ. Nonobvious obstructive meibomian gland dysfunction. Cornea. 2010;29(12):1333-45.
25. Millar TJ, Mudgil P, Butovich IA, Cowell BA. Phospholipids in the human meibomian gland secretion. Ophthalmic Res. 2011;46(4):193-9.

26. Bancroft JD, Gamble M. Theory and Practice of Histological Techniques. 6th ed. Edinburgh: Churchill Livingstone; 2008.
27. Luna LG. Manual of Histologic Staining Methods of the Armed Forces Institute of Pathology. 3rd ed. New York: McGraw-Hill; 1968.
28. Arita R, Itoh K, Inoue K, Amano S. Noncontact infrared meibography to document age-related changes of the meibomian glands in a normal population. Ophthalmology. 2008;115(5):911-5.
29. Tomlinson A, Bron AJ, Korb DR, Amano S, Paugh JR, Pearce EI, et al. The international workshop on meibomian gland dysfunction: report of the diagnosis subcommittee. Invest Ophthalmol Vis Sci. 2011;52(4):2006-49.
30. Mishima S, Maurice DM. The oily layer of the tear film and evaporation from the corneal surface. Exp Eye Res. 1961;1(1):39-45.
31. Green-Church KB, Butovich I, Willcox M, Borchman D, Paulsen F, Barabino S, et al. The international workshop on meibomian gland dysfunction: report of the subcommittee on tear film lipids and lipid-protein interactions in health and disease. Invest Ophthalmol Vis Sci. 2011;52(4):1979-93.
32. Baudouin C, Messmer EM, Aragona P, Benitez del Castillo J, Bitter T, Boboridis KG, et al. Revisiting the vicious circle of dry eye disease: a focus on the pathophysiology of meibomian gland dysfunction. Br J Ophthalmol. 2016;100(3):300-6.
33. McCulley JP, Shine WE. Changing concepts in the diagnosis and management of blepharitis. Cornea. 2000;19(5):650-8.
34. Parfitt GJ, Xie Y, Geyfman M, Brown DJ, Jester JV. Absence of ductal hyaluronan improves mouse meibomian gland function and reduces corneal disease. Am J Pathol. 2013;182(5):1891-9.
35. Craig JP, Nichols KK, Akpek EK, Caffery B, Dua HS, Joo CK, et al. TFOS DEWS II definition and classification report. Ocul Surf. 2017;15(3):276-83.
36. Korb DR, Blackie CA. Meibomian gland diagnostic expressibility: correlation with dry eye symptoms and gland location. Cornea. 2008;27(10):1142-7.
37. Maskin SL. Intraductal meibomian gland probing relieves symptoms of obstructive meibomian gland dysfunction. Cornea. 2010;29(10):1145-52.
38. Ibrahim OM, Matsumoto Y, Dogru M, Adan ES, Wakamatsu TH, Nojima T, et al. In vivo confocal microscopy evaluation of meibomian gland dysfunction in atopic-keratoconjunctivitis patients. Ophthalmology. 2012;119(10):1961-8.
39. Ngo W, Srinivasan S, Schulze M, Jones L. Repeatability of grading meibomian gland dropout using two infrared systems. Optom Vis Sci. 2014;91(5):539-49.
40. Schirmer KE. Meibomian glands and contact lens wear. Br J Ophthalmol. 1966;50(1):41-5.